Winds on Horizontal Scans from Doppler Lidar during T-REX

Aditya Choukulkar[1*], Ronald Calhoun[1], Brian Billings[2], and James Doyle[3]

[1] *Environmental Remote Sensing Group,*
Arizona State University, Tempe, AZ

[2] *National Research Council, Monterey, CA.*

[3] *Mesoscale Modeling Section,*
Naval Research Laboratory, Monterey, CA

Introduction

Flow in complex terrain particularly mountain valleys is important for several reasons. Flows in mountain valleys show interesting features over a wide range of scales due to turbulence generated by the interaction with the terrain and mountain slopes. An understanding of the fluid mechanics behind such flows would aid in a variety of applications, for example, for dispersion of pollutants and particulate matter in valleys, or wind farm characterization in complex terrain. In addition, rotors formed in mountain valleys have been responsible for numerous aeronautical accidents (Kahn *et al*. 1997) and hence need to be properly understood to prevent such incidents.

Lidar remote sensing techniques offer significant advantages for conducting these types of studies due to its ability to obtain observations with high enough spatial and temporal resolution to characterize transient fluid dynamical features (see, for example; Banta *et al*., 1999). In addition, the ability of Doppler lidar to perform programmable configurations of horizontal and vertical scans allows study of three-dimensional flow structures. There are several studies that make use of vertical lidar scans to study the flow on vertical cross-barrier planes during the Terrain-induced Rotors EXperiment (TREX) (see Hill *et al*., 2010 and Weissmann *et al*., 2009). Hill *et al*., (2010) made use of intersecting vertical lidar scans to track and characterize mountain-induced rotors and other flow structures in clear air. Weissmann *et al*., (2009) calculated the vorticity in the vertical 2-dimensional plane using continuity to derive the velocity component perpendicular to the line of sight. In this paper, a vector retrieval method based on optimal interpolation, recently adapted from the radar processing community for Doppler lidar (see Xu *et al*., 2006; Kongara *et al*., 2010), is used to educe the velocity vectors on horizontal lidar scans and study the horizontal flow structure. In addition, results from the Naval Research Laboratory's Coupled Ocean/Atmosphere Mesoscale Prediction System (COAMPS®) are also presented.

Experimental Setup

The Terrain Induced Rotor Experiment (TREX) was a study carried out in the Owens Valley of the Sierra Nevada mountain range to study the formation of rotors and study flow in complex terrain. A detailed description of the TREX campaign is given by Grubisic *et al*. (2008). The main objective of this study was to improve the understanding and predictability of the mountain-waves, rotors and boundary layer

* Presenting author, Email: achoukul@asu.edu, Ph: 480-727-8439

flow in complex terrain. This campaign was carried out for a period of two months from March 2006 to April 2006. The terrain surrounding the Owens Valley is complex and known to induce rotors and recirculations. The Owens Valley is approximately 100 km long and is oriented nearly north-south. It is surrounded by the Sierra Nevada Mountains on the west and the Inyo mountains on the east. The valley floor is approximately ten kilometers wide near Independence, CA, and this area is known for the formation of rotors and other complex flows.

A network of *in situ*, ground-based and airborne instruments were deployed by various organizations (Grubisic *et al*., 2008) to make measurements of the flow structure in the valley. Among the ground-based instruments were two Doppler lidars, one from Arizona State University (ASU) and one from the Deutsches Zentrum für Luft-und Raumfarht (DLR, German Aerospace Center) both *WindTracer* type, built by *Lockheed Martin Coherent Technologies, Inc*. The two lidars were placed approximately 2.9 km apart and performed scans which frequently intersected, thus allowing the possibility of dual Doppler analysis. The DLR lidar was located at 36°47'43.33"N, 118°12'28.74"W at an elevation of 1242 m above msl (mean sea level) and the ASU lidar was located at 36°47'51.74"N, 118°10'32.06"W at an elevation of 1179 m above msl. The positions of the lidars and other instrumentation used in this analysis are shown in Figure 1. The difference in elevation of the two lidar is 63 m. The location of the lidars on a cross section of the terrain is shown in Figure 2.

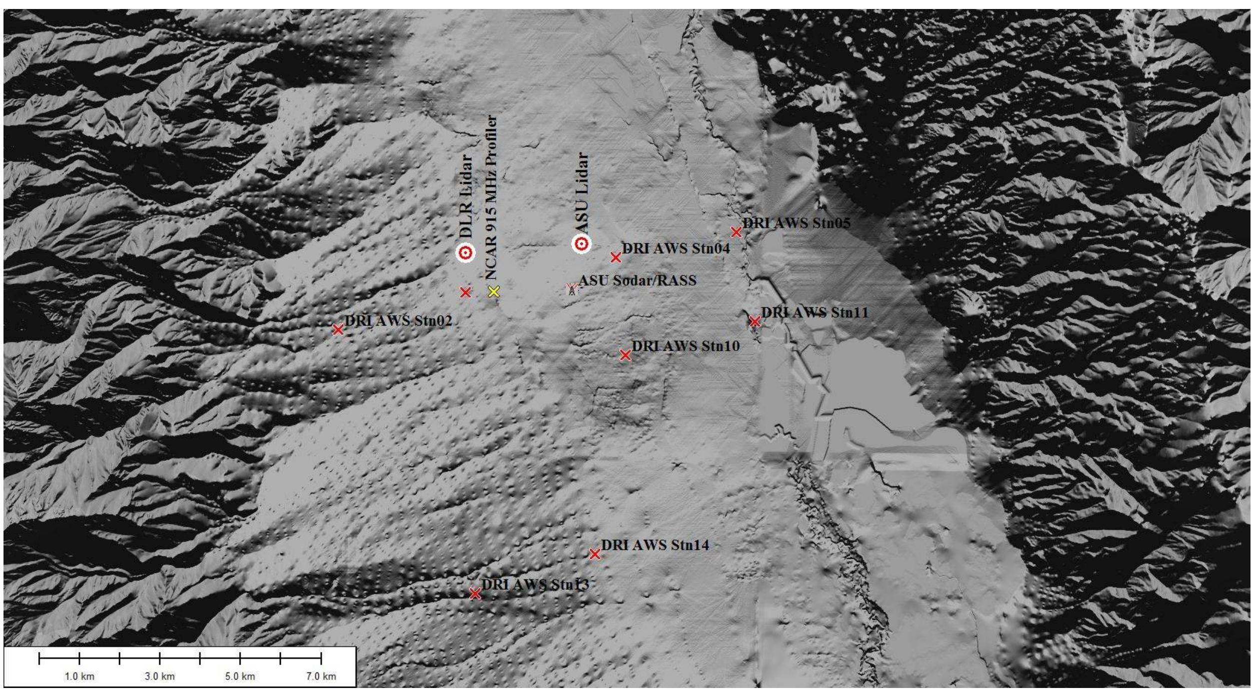

Figure 1. Locations of the instruments used in the analysis.

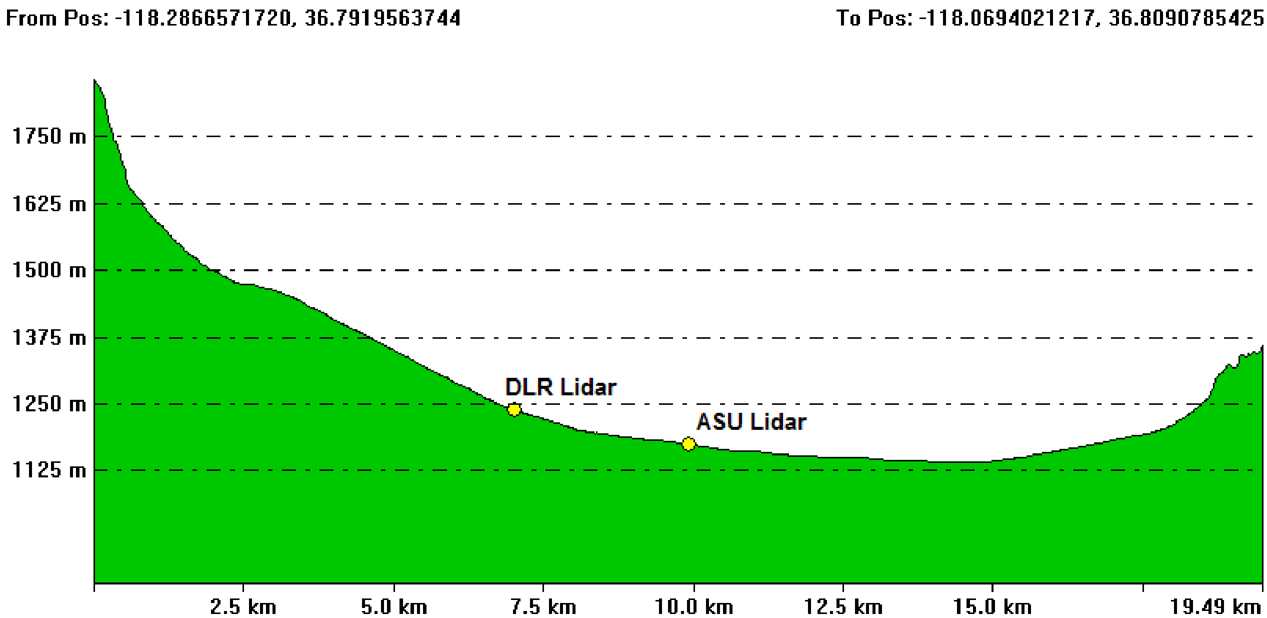

Figure 2. West to East cross-section of the terrain through the lidar positions.

Apart from the lidar, ASU had a Sodar/RASS setup at 36° 47' 14.85" N, 118° 10' 44.45" W for measuring vertical profiles of wind and temperature. The other instruments whose data were used in this paper are: 1) the NCAR (National Center for Atmospheric Research) 915 MHz profiler (located at 36° 47.2' N, 118° 12' W during this time period) and 2) the DRI (Desert Research Institute) Automatic Weather Station (AWS) network which took surface measurements at 16 locations.

In this paper, data collected by the lidars on March 27th 2006 are investigated. On this day both the ASU and the DLR lidar scanned a stack of PPI's (Plan Position Indicator scans) at elevation angles ranging from 0° to 26° with horizontal steps of 2°. The DLR lidar scanned from an azimuth angle of 31° to 119°, measured clockwise from north, while the ASU lidar scanned from 127° to 219°, measured clockwise from north. The time period of the observations was during the early morning of March 27th from 1030 to 1230 UTC (0230 to 0430 local time). This time period was selected because of complex, converging flow patterns observed in the Doppler lidar data. It is observed that there was a change in the direction of flow with height and evidence of a cross-valley flow impinging from the west.

Retrieval Method

The Doppler lidar measures only the radial component of the velocity and hence requires additional analysis to retrieve wind vector fields. There are a variety of techniques to accomplish the vector retrievals, ranging from very simple methods such as the Velocity Azimuth Display (VAD, see Browning and Wexler 1968; Gal Chen 1992) to more intricate methods such as four-Dimensional Variational Data Assimilation (4DVAR, see for example, Newsom *et al.*, 2004 and Lin *et al*. 2008). The VAD methods are simple and efficient, but the wind vector retrievals are spatially averaged. Since a major strength of modern 3D scanning Doppler lidar is high temporal and spatial resolution, simple spatially averaged methods do not fully realize the data potential. The methods based on variational analysis are computationally intensive, requiring solutions to adjoint-methods (Newsom *et al.* 2004; Xia *et al*. 2008; Lin *et al*. 2008) and are more resource expensive for frequent use such as for rapid nowcasting.

To bridge the gap between these available methods, a vector retrieval algorithm based on data assimilation technique put forward by Xu et al. (2006; 2007) was adapted to work with Doppler lidar data (Kongara *et al*., 2010). This technique works by importing observations into a prediction model to find an analysis field that is most consistent with the observations. The analysis field is defined as background plus the weighted innovation.

$$\text{Analysis} = \text{Background} + \text{W} \times \text{Innovation}$$

where, Innovation = Observation – Background, and W is the weighting function which is a combination of the background error covariance matrix and the observation error covariance matrix (see Xu & Gong, 2003).

This weighting is estimated based on a Bayesian standpoint (Lorenc 1981; Daley 1991) which takes into account the possibility of errors in the observations. In this method, we use probabilities to estimate the confidence in knowledge of past data (background) and these probabilities are modified in light of new knowledge (observations). The new analysis estimate is arrived at by adding an analysis increment to the background. This analysis increment is arrived at by minimizing the following cost function

$$J = \Delta \boldsymbol{a}^{\mathsf{T}} \mathbf{B}^{-1} \Delta \boldsymbol{a} + \left(\Delta \boldsymbol{a} - \boldsymbol{d}\right)^{\mathsf{T}} \mathbf{R}^{-1} \left(\Delta \boldsymbol{a} - \boldsymbol{d}\right)$$

where $\Delta \boldsymbol{a}$ is the analysis increment, given by

$$\Delta \boldsymbol{a} = \boldsymbol{x}^{\mathrm{b}} - \boldsymbol{x}$$

where $\boldsymbol{x}^{\mathbf{b}}$ is the background vector field and $\boldsymbol{x}$ is the analyzed vector field,

$\boldsymbol{d}$ is the innovation and

B and **R** are the background error covariance and observation error covariance matrices respectively.

Validation

To determine the accuracy of the retrieval algorithm several checks were made. First the dot product of the retrieved velocity vectors, both from the VAD and the OI algorithm, was taken along the beam direction to get back the radial velocity. This back-calculated radial velocity was compared with the original lidar retrieved radial velocity signal for agreement. Figure 3 shows the comparison of the originally measured radial velocity, from one range-ring, with the VAD retrieved and the OI retrieved radial velocity.

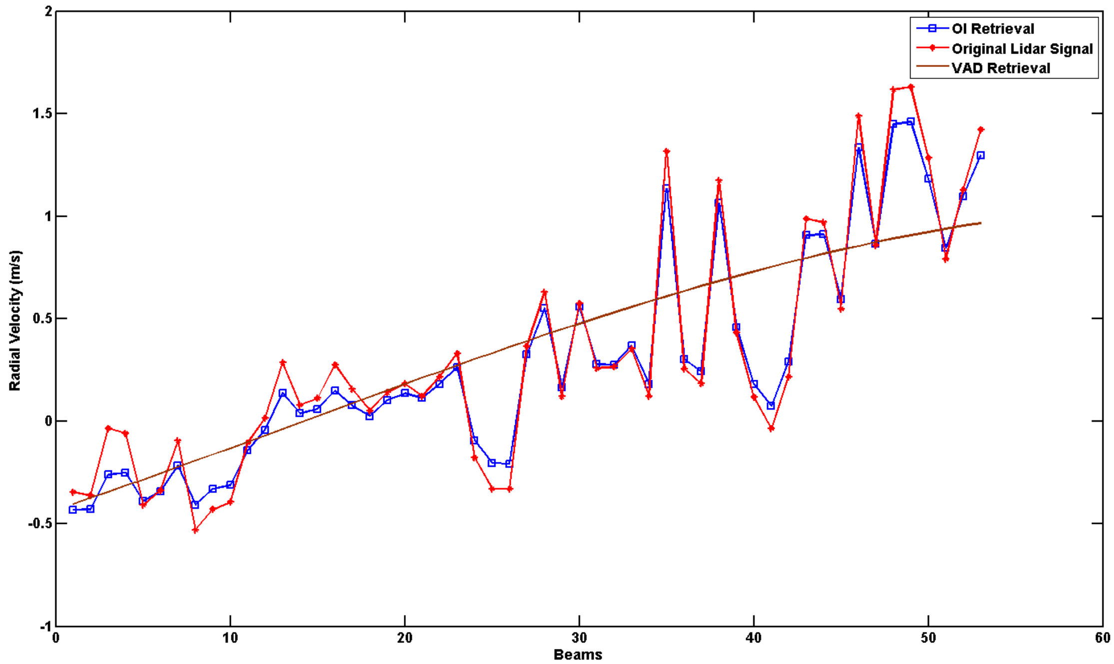

Figure 3. Comparison of VAD retrieved radial velocity and OI retrieved radial velocity with the original lidar measured radial velocity.

As can be seen from the Figure 3, the VAD estimates the mean velocity field and all the local information is lost. The OI method on the other hand is able to keep most of the local information and the retrieval compares very well with the originally measured radial velocity. Further checks are made comparing the retrievals with other *in-situ* instruments in the valley for agreement.

COAMPS Retrievals

The Naval Research Laboratory's Coupled Ocean/Atmosphere Mesoscale Prediction System (COAMPS®, Hodur 1997) is a fully compressible, non-hydrostatic model which solves the governing equations using a centered-in-time finite difference scheme on an Arakawa-C grid and a sigma vertical coordinate system. The model uses a full suite of physical parameterizations to include the effects of subgrid-scale turbulence and boundary layers, radiative heating and cooling, cumulus convection, and cloud microphysics. The turbulence parameterization uses a 1.5 order, level 2.5 Mellor and Yamada (1982) scheme that computes boundary layer depth, turbulent mixing length, Richardson number, and eddy coefficients to explicitly predict the change in TKE.

The lateral boundary conditions for these simulations are taken from the Navy Operational Global Atmospheric Prediction System (NOGAPS), which also provides the first-guess field for the initial conditions. Observations are assimilated into the initial conditions using the NRL Atmospheric Variational Data Assimilation System (NAVDAS). There are four nested domains with horizontal resolutions of 9-, 3-, 1-, and 0.33 km. The simulations was started from the NOGAPS analysis at 00 UTC 27 March 2006 and iterated for 24 hours.

Observations

The flow in the Owens Valley during the time period from 1030 UTC to 1230 UTC (0230 hr to 0430 hr local time) shows interesting behavior. The upper layer flow observed at a height of ~5000 m during this time, as measured by the NCAR DBS profiler (see Figure 4) is flowing approximately from the south-west to the north-east. The COAMPS result on a 500 m height terrain following surface shows a similar result (see Figure 5). It is also seen that the flow within the valley is generally up-valley. This is due to the fact that the direction of the wind being approximately aligned with the valley axis, there is high probability of this flow being channeled into the valley. On the other hand, the stable night-time conditions present would favor down-valley and down-slope flows within the valley.

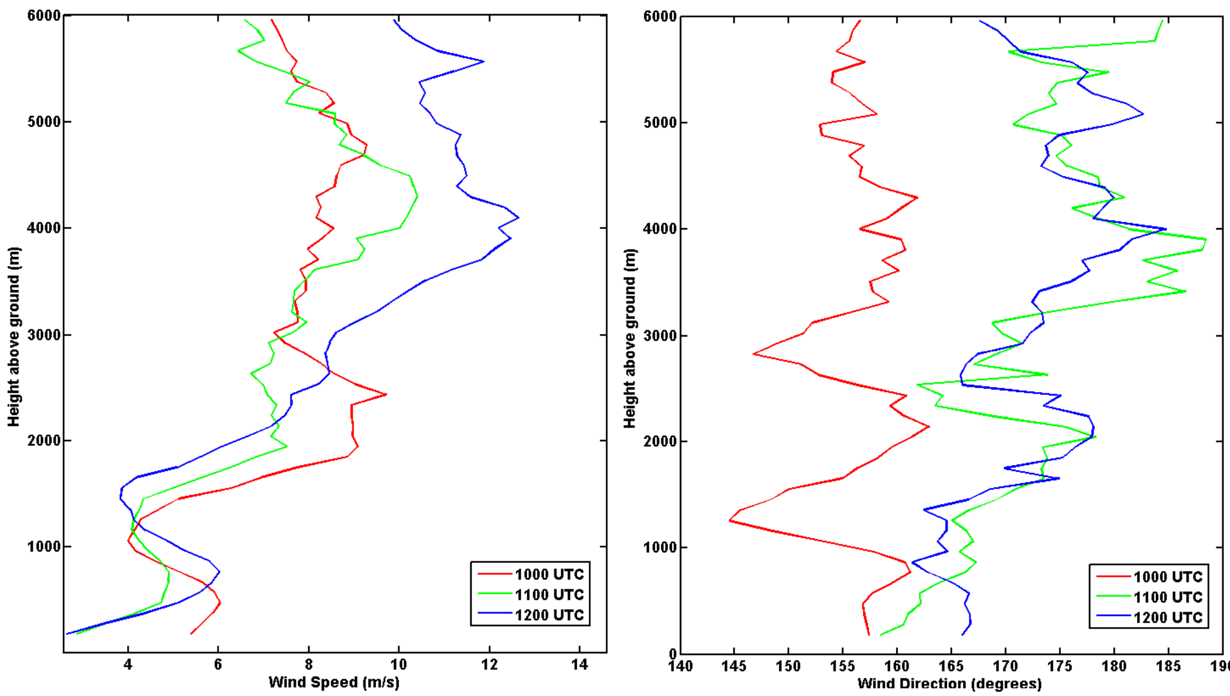

Figure 4. Vertical profiles of horizontal wind speed and wind direction profiles as measured by the NCAR DBS 915 MHz profiler.

A look at the vector retrievals from the ASU lidar indeed shows a presence of both these types of flows. Figure 6 shows the vertical velocity vectors retrieved from the stack of ASU lidar PPI scans. The vector plot is formed by binning the vectors retrieved from the OI method for the low elevation angle scans and the VAD for the high elevation angle scans into 20 m height bins. Due to the difference in the nature of the retrieval methods the spatial averaging is different for the lower levels and the higher levels. On the lower levels, there is no averaging in the azimuth direction while the averaging is about 1.5 km in the radial direction. On the lower level, retrievals centered on the beam closest to the NCAR profiler are used, for the purposes of comparison. Consequently, the given profiles are further away from the DRI AWS, though still remarkably good, as seen below. Vectors from the first 10-15 range-gates of a given beam are used for binning depending on the elevation angle of the scan. While on the higher level, since VAD is used for vector retrieval, there is spatial averaging in the radial as well as azimuth direction. This spatial averaging on the upper (VAD) levels is of the order 3 km in the azimuthal direction and 1.5 km in the radial direction.

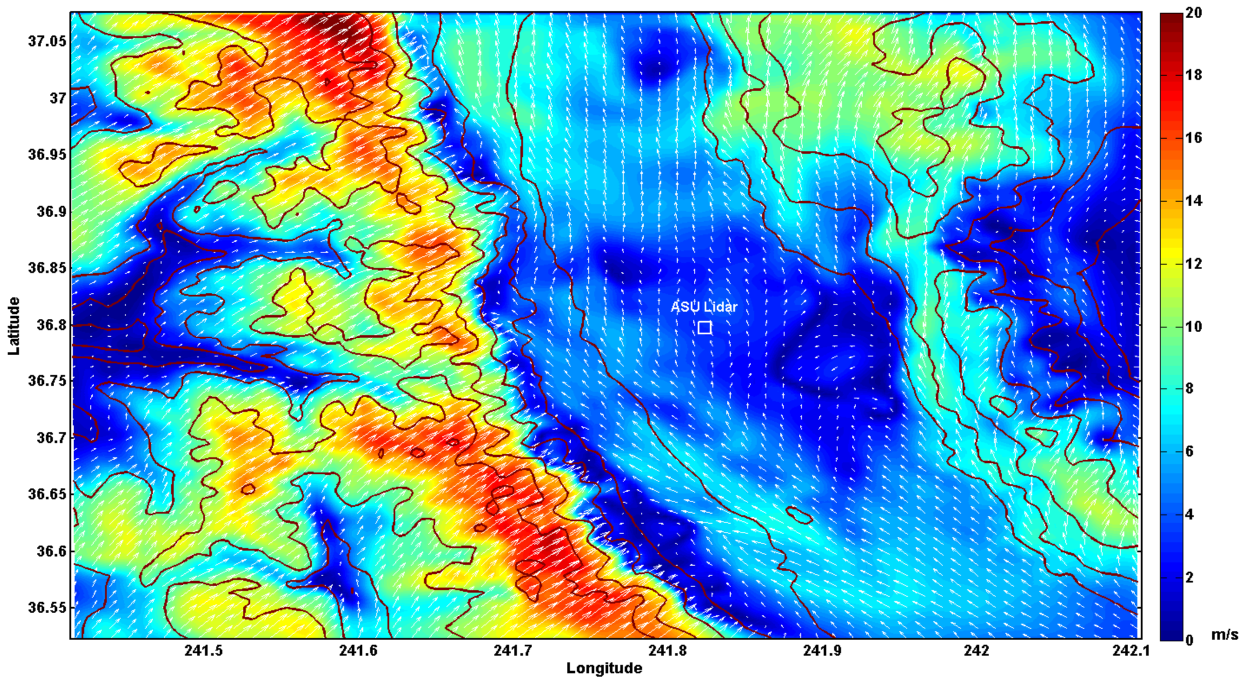

Figure 5. Results from COAMPS run on a 500 m height terrain following surface.

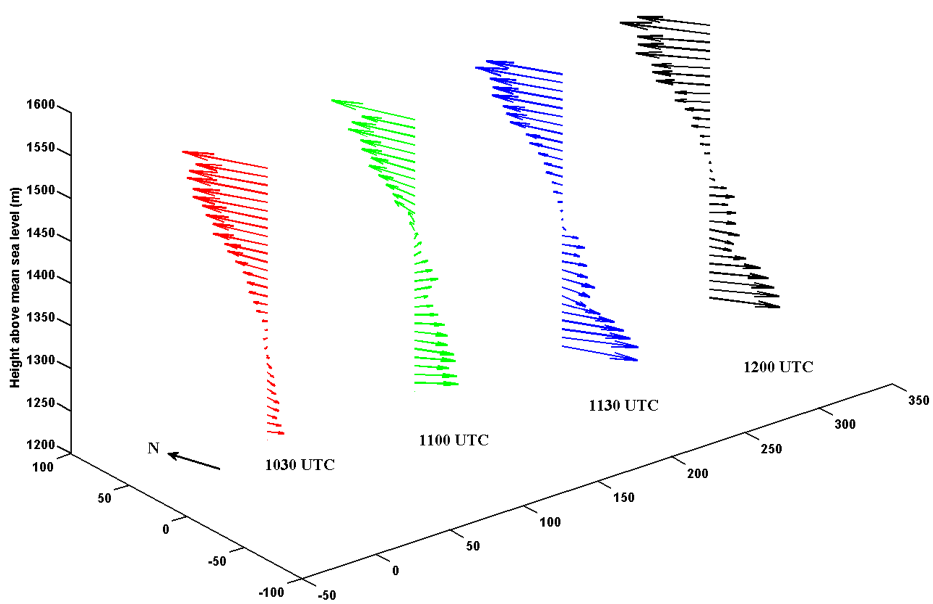

Figure 6. Vertical profiles of horizontal velocity vectors from ASU lidar showing the opposing flow structure in the Owens Valley.

It can be seen from Figure 6 that the lower level flow is down-valley while the upper level flow is up-valley. Also, it can be seen that the lower down-valley flow increases in strength and height with time. The reason for this is still unclear and more investigation is required before reasons for this can be ascertained.

To ascertain the accuracy of these retrievals, they were compared with measurements from nearby profilers and surface station measurements. Figures 8 and 9 show the comparisons of the wind speeds and wind directions retrieved from the lidar with those measured by the NCAR DBS profiler and the DRI AWS surface station 4. The heights above mean sea level are used to plot the values to take into account differences in terrain heights. It can be seen that the wind speed and wind directions measured by the lidar, the NCAR DBS profiler and the DRI AWS station are in good agreement. It also confirms the two layer opposing flow pattern observed by the lidar. Note that the direction of the wind at 1030 UTC is measured to be ~260 degrees clockwise from north at the lower levels given in the Figure 6. That is, winds were flowing cross-valley from the west to the east during this time. This cross-valley current could be due to the down-slope winds intruding into the flow along the valley axis. This can be seen from the results of the COAMPS run on a 10 m terrain following surface for this time (see Figure 7).

Since the cross valley flow at 1030 UTC is flowing from the west to the east, it can be observed best from the DLR lidar retrievals. Figure 8 shows the retrievals from the DLR lidar from 1029 UTC to 1101 UTC. It can be seen that there is initially a cross-valley flow meeting the low level down-valley flow leading to complex mixing at their meeting point. This cross-valley flow decreases in magnitude with time and is finally replaced by the generally down-valley flow.

We see that the cross-valley flow seems to be a transient event and dies out quickly to be replaced by a generally down-slope flow. This could most probably be due to the fact that as cooling continues through the night, the height of the nocturnal boundary layer increases strengthening the down-valley flow. Further analysis is required to ascertain the reasons for this flow behavior.

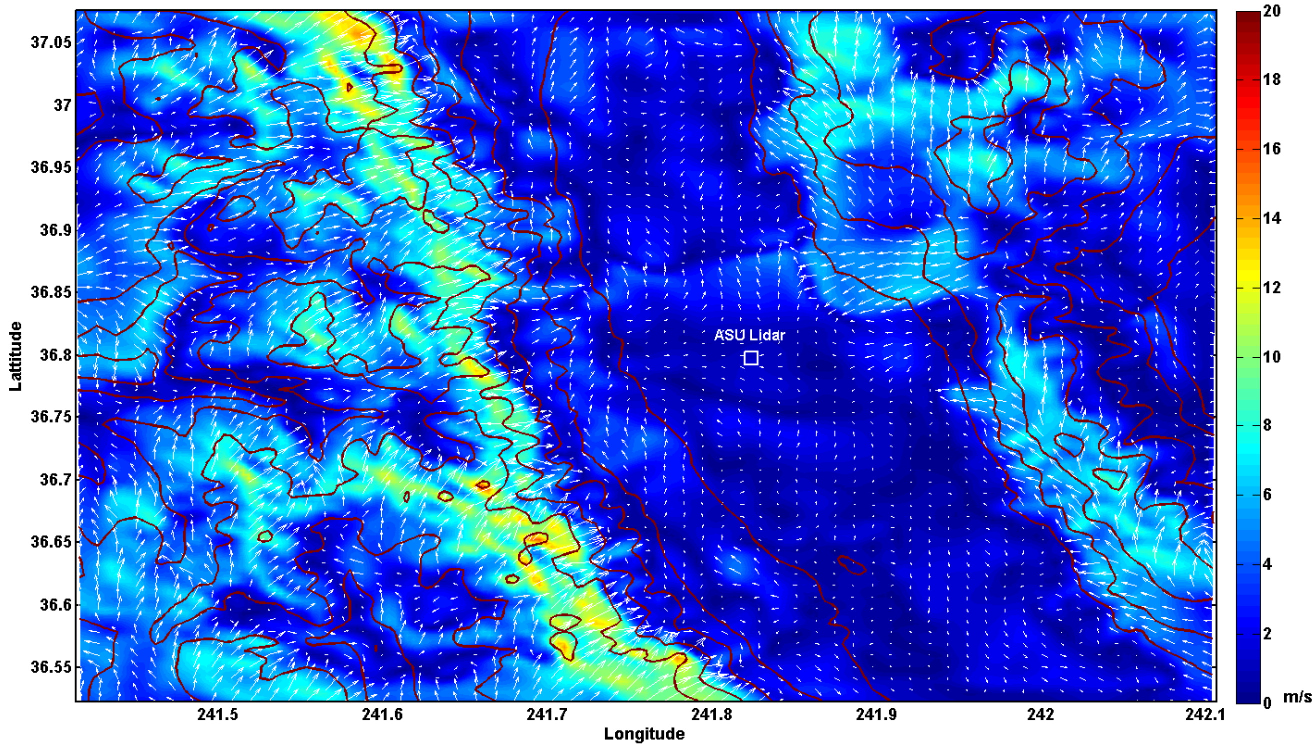

Figure 7. Results from COAMPS run on a 10 m height terrain following surface.

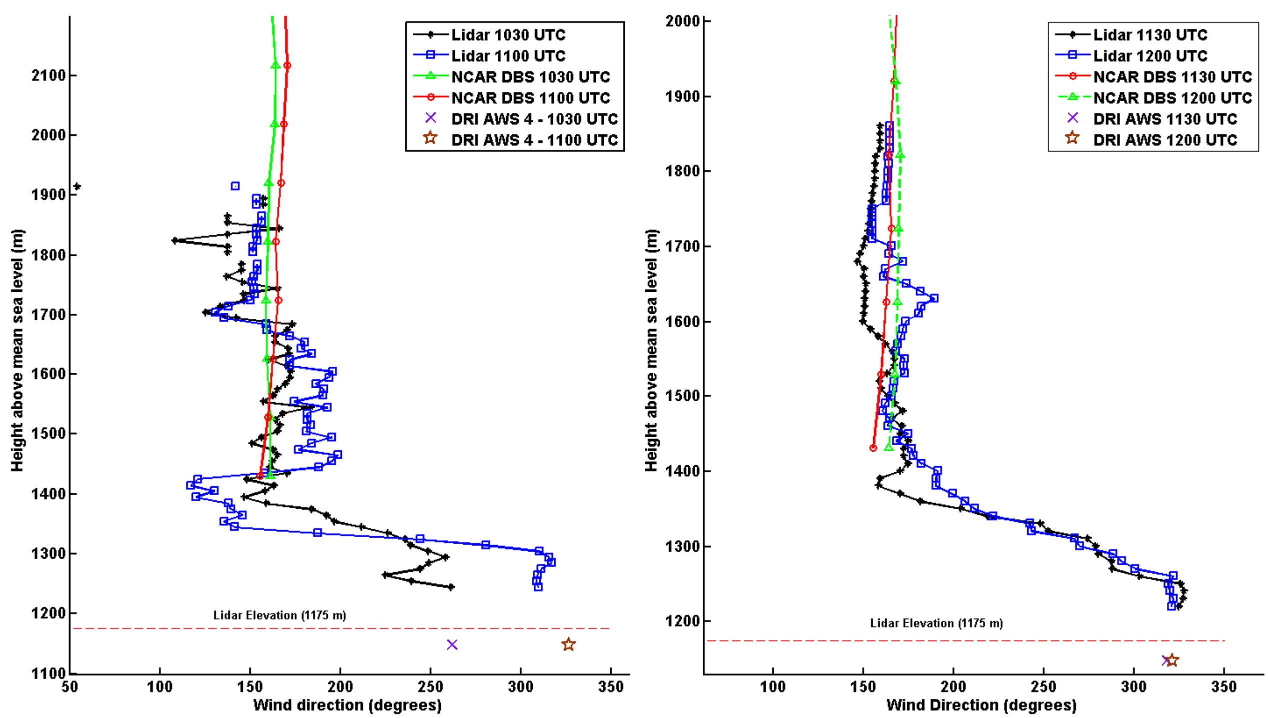

Figure 8. Comparison of wind directions measured by lidar, NCAR DBS profiler and DRI AWS.

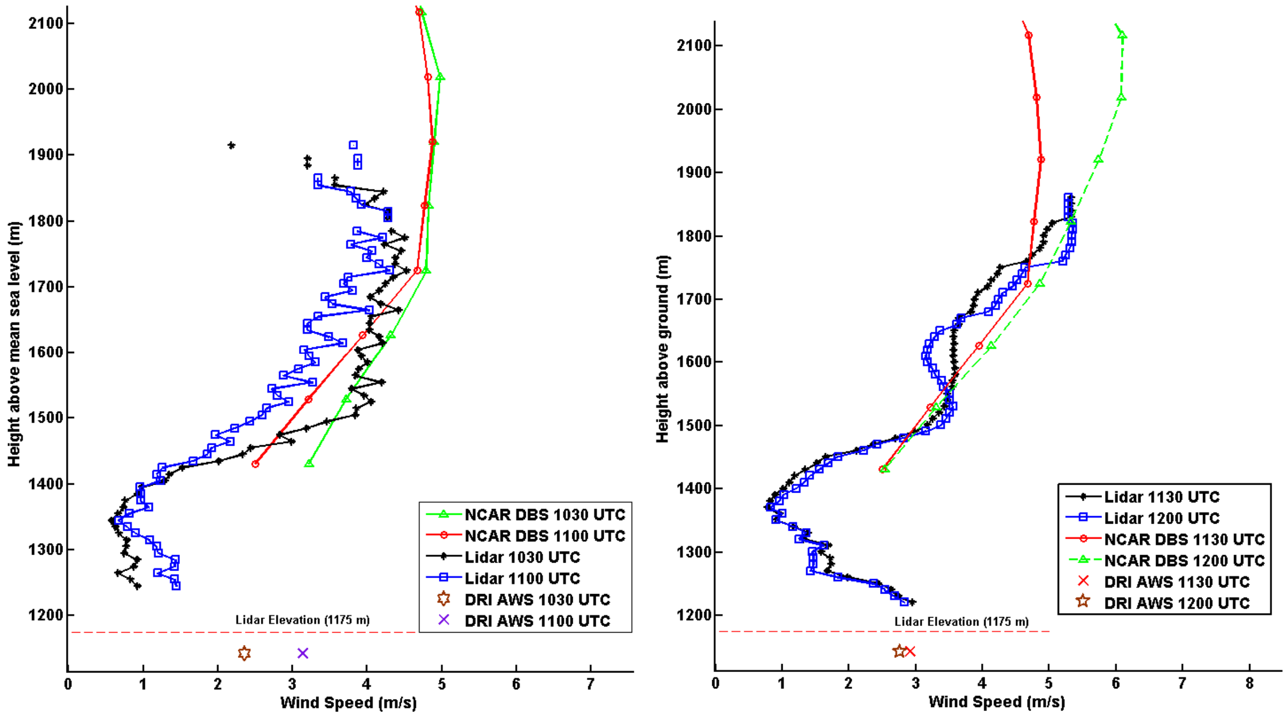

Figure 9. Comparison of wind speeds measured by the lidar, NCAR DBS profiler and DRI AWS.

Conclusions

A vector retrieval algorithm based on Optimal Interpolation is used to analyze the horizontal flow structure in the Owens Valley during the TREX field experiment. The present analysis showcases the ability of lidar based remote sensing techniques to analyze flow in complex terrain. It is found that a double layer flow structure exists during the early morning period of Mar 27. The lower level flow is expected to be thermally driven, while the upper layer flow is expected to be synoptic flow channeled into the valley.

There are still unanswered questions about this flow. The time of origin and nature of the cross-valley flow is not known yet. It is not known how fast it flows down-valley and what is the height and depth of this current. The data collected by the ASU and DLR lidars can help answer these questions. Using the stack of PPI scans, the depth and origin of the cross-valley flow can be estimated. In addition to this, the results obtained from lidar analysis are being compared with results from a COAMPS run for this time period to understand the strengths and weaknesses of each of these approaches.

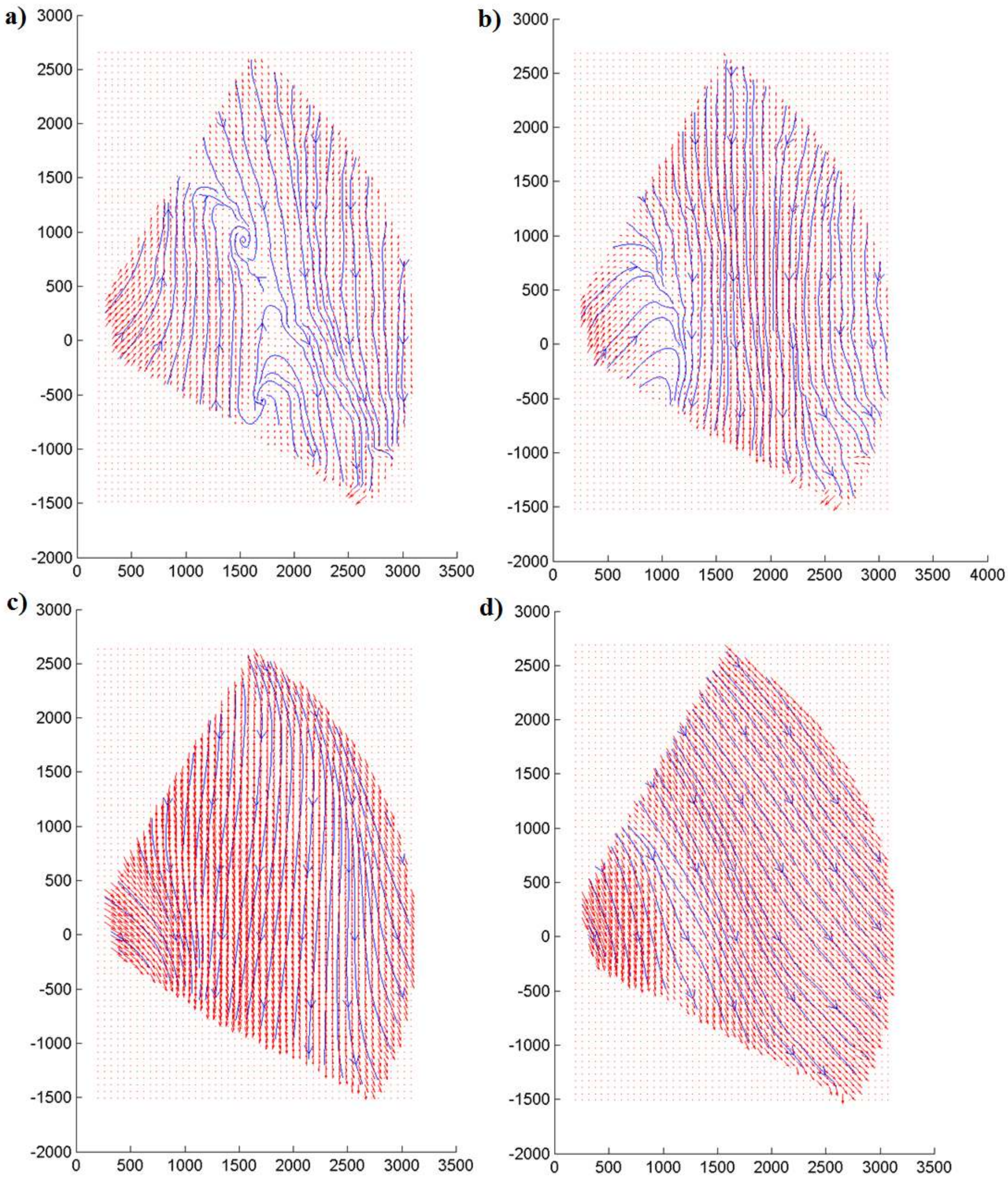

Figure 8. OI retrievals from DLR 0 degree elevation scan showing cross-valley jet mixing and then decreasing in strength to be replaced by down-valley flow. a) 1029 UTC b) 1045 UTC c) 1051 UTC d) 1101 UTC.

Acknowledgement

The authors recognizes the support of the Army Research Office, sponsor awards W911NF0410146 and W911NF0710137 (Program Officer: Walter Bach) and the NSF grant 0522307 (Program Officer: Stephan P. Nelson) which made this work possible. The authors are also grateful for the support of the Office of Naval Research Summer Faculty Research Program during summer of 2010. The authors would like to thank National Center for Atmospheric Research (NCAR), the DLR, and the Desert Research Institute (DRI) for allowing the use of their data which made this study possible. The AWS data was gathered as part of the Terrain-induced Rotor Experiment (T-REX). The primary sponsor of T-REX was the US National Science Foundation. The acquisition of this data was carried out by the Desert Research Institute (DRI) team (PI Grubišić) funded in part by NSF grants ATM-0242886 and ATM-0524891 to DRI.

References

Banta R.M., Darby L.S., Kaufmann P., Levinson D.H., Zhu C-J., 1999: Wind-flow patterns in Grand Canyon as revealed by Doppler lidar. *Journal of Applied Meteorology*. **38**, 1069-1083

Browning, K. A., R. Wexler, 1968: The determination of kinematic properties of a wind field using Doppler radar. *Journal of Applied Meteorology*, **7**, 105–113.

Daley, R., 1991: Atmospheric Data Analysis. Cambridge University Press.

Gal-chen, T., M. Xu, W. Eberhard, 1992: Estimations of atmospheric boundary layer fluxes and other turbulence parameters from Doppler lidar data. *Journal of Geophysical. Research*, **97**, 409-418.

Grubisic V., and co-authors, 2008: The Terrain-Induced Rotor Experiment: An overview of the field campaign and some highlight of special observations. *Bulletin of the American Meteorological Society*, **89**, 1513-1533.

Hill M., Calhoun R., Fernando HJS., Wieser A., Bornbrack A., Weissmann M., Mayr G., Newsom R., 2010: Coplanar Doppler lidar retrievals of rotors from T-REX. *Journal of the Atmospheric Sciences*. **67**, 713-729.

Kahn B. H., W. Chan, P. F. Lester, 1997: An investigation of rotor flow using DFDR data. *Proc. Seventh Conf. on Aviation, Range, and Aerospace Meteorology*, Long Beach, CA, American Meteorological Society, 206–210.

Kongara S., Calhoun R., Choukulkar A., Boldi MO., 2010: Velocity retrievals for coherent Doppler lidar. *International Journal of Remote Sensing*, In Press.

Lin, C., Q. Xia, R. Calhoun, 2008: Retrieval of urban boundary layer structures from Doppler lidar data. Part II: Proper orthogonal decomposition. *Journal of Atmospheric Sciences*, **65**, 21-42.

Lorenc, A., 1981: A Global three dimensional multivariate statistical analysis system. *Monthly Weather Review*, **109**, 701-721.

Newsom, R., T. Chai, C. Lin, 2004: Retrieval of Microscale Flow Structures from High Resolution Doppler Lidar Data Using an Adjoint Model. *Journal of Atmospheric Sciences*, **61**, 1500-1520.

Weissmann M., Dornbrack A., Doyle JD., 2009: Vorticity from line-of-sight lidar velocity scans. *Journal of Atmospheric and Oceanic Technology*, **26**, 2683-2690.

Xia, Q., C. Lin, R. Calhoun, R. Newsom, 2008: Retrieval of urban boundary layer structures from Doppler lidar data. Part I: Accuracy assessment. *Journal of Atmospheric Sciences*, **65**, 3-20.

Xu, Q., and J. Gong, 2003: Background error covariance functions for Doppler radial-wind analysis. *Quarterly Journal of the Royal Meteorological Society*, **129**, 1703-1720.

Xu, Q., K. Nai, L. Wei, 2007: An Innovation Method for Estimating Radar Radial-Velocity Observation Error and Background Error Covariances. *Quarterly Journal of the Royal Meteorological Society*, **133**, 407-415.

Xu, Q., S. Liu, M. Xue, 2006: Background Error Covariance Functions for Velocity Wind Analysis using Doppler Radar Radial-Velocity Observations. *Quarterly Journal of the Royal Meteorological Society*, **132**, 2887-2904.

Hodur, R. M., 1997: The Naval Research Laboratory Coupled Ocean/Atmosphere Mesoscale Prediction System (COAMPS). *Monthly Weather Review*, **125**, 1414-1430.

Mellor, G. L., T. Yamada, 1982: Development of a turbulence closure model for geophysical fluid problems. *Review Geophysics and Space Physics*, **20**, 851-875.